# The phase stability, mechanical and electronic properties of CsCl-type intermetallic: $Ti_{50}TM_{50}$ (TM = Ni, Ru and Pd), a first-principles approach

**B.S. Ngobe**[1, 2]**, M.J. Phasha**[1]**, RG Diale**[1] **and MP Molepo**[2]

[1] Advanced Materials Division, MINTEK, Randburg, South Africa

[2] School of Physics, University of the Witwatersrand, Johannesburg, South Africa

E-mail: `Bonganing@mintek.co.za and 2623288@students.wits.ac.za`

**Abstract**. Most Ti-based CsCl-type compounds solidify to an ordered B2 phase at high temperature and upon cooling they transform martensitically to lower temperature phases. In this work, phase stability, mechanical and electronic properties of three CsCl-type intermetallics $Ti_{50}TM_{50}$ (TM=Ni, Ru and Pd) computed using density functional theory (DFT) based on the first-principles technique are reported. The obtained lattice parameters are in good agreement with experimental results, an indication that the computational parameters used can be reliable to calculate other physical properties. Enthalpy of formations ($\Delta H_F$) and density of states (DOS), which are used to evaluate the thermodynamic stability of the compound, were calculated from the geometrically optimized crystal structures. High negative heat of formation (-0.75 eV/atom) was obtained for $Ti_{50}Ru_{50}$ phase, and its Fermi level was found to coincide with the centre of the pseudogap demonstrating high stability and resistance to phase transition amongst the investigated compounds. The primary elastic constants ($C_{11}$, $C_{12}$ and $C_{44}$) and shear elastic coefficient ($C'$) for cubic crystals were calculated. $Ti_{50}Ru_{50}$ and $Ti_{50}Ni_{50}$ complied with the mechanical stability while $Ti_{50}Pd_{50}$ did not comply. Furthermore, $Ti_{50}Ru_{50}$ was found to exhibit only positive frequencies, while $Ti_{50}Pd_{50}$ and $Ti_{50}Ni_{50}$ exhibit both positive and negative frequencies signifying phase transition to lower temperature phases.

## 1. Introduction

Nitinol is a commercial name given to equiatomic TiNi intermetallic compounds [1-2]. It is part of intermetallic compounds that form instantly from a molten liquid containing atoms of Group 10 (Ti, Zr and Hf) plus that of Group 10 metals of the periodic table [3]. On cooling, it crystallizes to an ordered B2 of Cesium Chloride (CsCl-type) near the equiatomic compositional range [1, 4-5]. B2 is a high symmetry austenite phase that exists at high temperatures, and upon further cooling, it undergoes a diffusionless solid-to-solid structural change to a low symmetry martensitic phase [1-2, 6-7]. Structural alloys that conform to this phenomenon are called shape memory alloys (SMA) [1, 4-5]. These are a unique class of materials with an ability to remember previous crystal arrangement and properties, and currently enjoy a wide range of structural applications in medical and engineering materials [1-2].

Apart from its excellent shape memory effect and pseudo-elasticity, Nitinol has its drawbacks such as its low-temperature application that hinders it as an SMA for high temperature (HTSMA) applications that exceed 100°C [1-2]. On the other hand, Platinum group metals (PGMs) which are located in Group 10 of the periodic table of elements, form the B2 phase with Group 4 metals near 50:50 atomic percentage [3, 8]. Their nobleness and high-temperature stability enable PGMs as the candidate of choice for high-temperature applications [9]. Ti-PGMs based such as $Ti_{50}Pt_{50}$ and $Ti_{50}Pd_{50}$ are currently explored as potential candidates for high-temperature applications, such as for aerospace engines [4-5, 10]. Previous studies demonstrated and reported that some of the Ti-PGMs based compounds such as $Ti_{50}Ru_{50}$ and $Ti_{50}Os_{50}$ do not have a shape memory effect (SME); their B2 phase remains ordered and stable down to room temperature [11].

In this study, we report work carried out using first-principles calculations based on density functional theory (DFT) to compute the phase stability, mechanical and electronic properties of the three investigated $Ti_{50}TM_{50}$ (TM = Ni, Ru and Pd) compounds.

## 2. Computational methods

The calculations reported here were carried out using first-principles density functional theory (DFT) as implemented in Cambridge Serial Total Energy Package (CASTEP) code [12, 13]. The ultra-soft pseudopotentials (USSPs) were used to model the electron-ion interactions [14]. The electron-exchange correlation was described by the Perdew-Burke-Ernzerhof (PBE) functional of the generalized gradient approximation (GGA) [15, 16]. The energy cut-off of 500 eV and the k-points of 13×13×13 were used and found to be sufficient enough to converge the total energy of the investigated B2 compounds.

All the equilibrium B2 crystal structures were obtained through geometry optimization in the Brayden-Fletcher-Goldfarb-Shanno (BFGS) minimization scheme [17].

Figure 1 shows the schematic representation of the crystal structure used to carry the structural and thermodynamic, electronic and vibrational stability of the CsCl-type compounds reported in this research work. The lattice dynamics were computed via the linear response method as implemented in the CASTEP code.

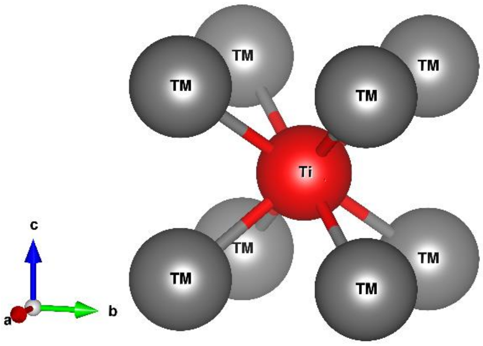

**Figure 1**. Schematic representation of B2 crystal geometry of $Ti_{50}TM_{50}$ (TM = Ni, Ru and Pd) used in this study work

## 3. Results and discussion

### 3.1. *Structural and thermodynamic properties*

Table 1 present the calculated lattice parameters and the formation enthalpies that were determined from the relaxed crystal geometries of the three investigated B2 compounds. The obtained lattice parameters of the investigated B2 compounds were found to be comparable to those reported by other authors [3, 18-20].

**Table 1**- Structural parameters of the investigated B2 crystal geometry

| **Crystal structure** | **Lattice parameters, a (*Å*)** | | **Formation enthalpies, ($\Delta H_F$) eV.atom$^{-1}$** | |
|---|---|---|---|---|
| | This work | Literature | This work | Literature |
| $Ti_{50}Ni_{50}$ | 3.01 | 3.02[18] | -0.382 | -0.357[23], -0.352[24] |
| $Ti_{50}Ru_{50}$ | 3.08 | 3.09[3, 19] | -0.75 | -0.743[8], -0.770[9] |
| $Ti_{50}Pd_{50}$ | 3.17 | 3.17[20] | -0.508 | -0.530[9], -0.511[23] |

Moreover, the phase stability of any compound can be deduced from the formation enthalpies ($\Delta H_F$) as expressed in Equation 1 [8, 21], and it is used to indicate the thermodynamic ability of a compound to be existent. A phase is said to be thermodynamically stable if $\Delta H_F$ is found to be negative, else the phase becomes less stable if less negative or unstable if found to be positive at 0 K [22].

$$\Delta H_F = \frac{1}{2}\left(E_{\boldsymbol{Bin}}^{Tot} - E_{Element}^{Ti} - E_{Element}^{TM}\right) \qquad (1)$$

where $E_{Bin}^{Tot}$ represents the total energy of the B2 compound, $E_{Element}^{Ti}$ and $E_{Element}^{TM}$ represent the elemental total energies of Ti and TM in their ground-state crystal structures. As presented in Table 1, all the investigated B2 compounds were found to be thermodynamically stable ($\Delta H_F < 0$), with $Ti_{50}Ru_{50}$ and $Ti_{50}Ni_{50}$, found to be the most and least thermodynamically stable compounds respectively. Again, the results reported here were found to be in accordance with results reported by other researchers [8-9, 23-24].

### *3.2. Elastic and Mechanical stability*

Elastic constants ($C_{ij}$) are part of the primary output parameters of first-principles calculations, as they provide a link between the mechanical and dynamic behaviour of crystals [25-26]. Key properties of materials such as physical and mechanical can be deduced from the elastic constants. B2 compounds consist of a simplest cubic form of a stiffness matrix, where the number of the independent elastic constants are reduced to three ($C_{11}$, $C_{12}$ and $C_{44}$) in the Voigt notation, and the shear elastic coefficient $C'$ for assessing the compound's prospect to undergo a phase transition at lower temperatures can be expressed as shown in Equation 2.

$$C' = \left(\frac{C_{11}-C_{12}}{2}\right) \qquad (2)$$

According to Born-Huang's dynamical theory [27-28], the mechanical stability criteria for B2 compounds can be determined by satisfying the criteria given by a set of expressions in Equation 3.

$$C_{11} > 0, C_{44} > 0, C_{11} - C_{12} > 0, C_{11} + 2C_{12} > 0 \qquad (3)$$

The crystal's mechanical stability decreases when closer to phase transition [29], where the tetragonal shear modulus ($C'$) becomes smaller than the monoclinic shear constant ($C_{44}$), which represents the stiffness of the crystal against shear. Table 2 present the elastic parameters of the investigated B2 compounds. Both $Ti_{50}Ru_{50}$ and $Ti_{50}Ni_{50}$ satisfied all the mechanical stability criteria as detailed in Equation 3, while $Ti_{50}Pd_{50}$ did not comply ($C_{11} < C_{12}$) with the above-mentioned criteria. This is an indication that this B2 compound is prone to undergo phase transition at lower temperatures.

**Table 2**. Elastics constants as well as their calculated modulus of elasticity for the investigated B2 compounds

| **B2 crystal** | **Elastic constants (GPa)** | | | |
|---|---|---|---|---|
| | **$C_{11}$** | **$C_{12}$** | **$C_{44}$** | **C'** |
| $Ti_{50}Ni_{50}$ | 206.7 | 138.7 | 47.1 | 34 |
| $Ti_{50}Ru_{50}$ | 396.1 | 122.5 | 82.7 | 136.8 |
| $Ti_{50}Pd_{50}$ | 148.5 | 164.0 | 51.5 | -7.8 |

### *3.3. Electronic and vibrational stability*

A compound is considered stable at 0 K if there are no soft modes along high symmetry directions in the Brillouin zone (BZ) [30]. And the presence of soft modes or negative frequencies indicates the instability of the crystal, an indication of the likelihood to undergo a phase transition, accompanied by lattice deformation [30-31].

Figure 2 represents the electronic properties of the investigated compounds, the phonon dispersion curves plotted along the selected Brillouin zone as well as their corresponding total density of states computed at 0 K. As can be seen, Figures 2 (a) and (b) show the phonon dispersion curves for $Ti_{50}Ni_{50}$ and $Ti_{50}Pd_{50}$ respectively, and both were found to consist of both positive (real) and negative (imaginary) vibrational frequencies. The imaginary frequencies are located between **X-R**, **G-R** and at **M** symmetry points, thereby making these compound's phases dynamically unstable, and an indication of phase transition at lower temperatures. Figure 2 (c) represents the phonon vibrational frequencies for $Ti_{50}Ru_{50}$ that were found to be real (positive) in all Brillouin directions, and this is a clear demonstration that this B2 phase is dynamically stable, with no prospect of phase transition at lower temperatures.

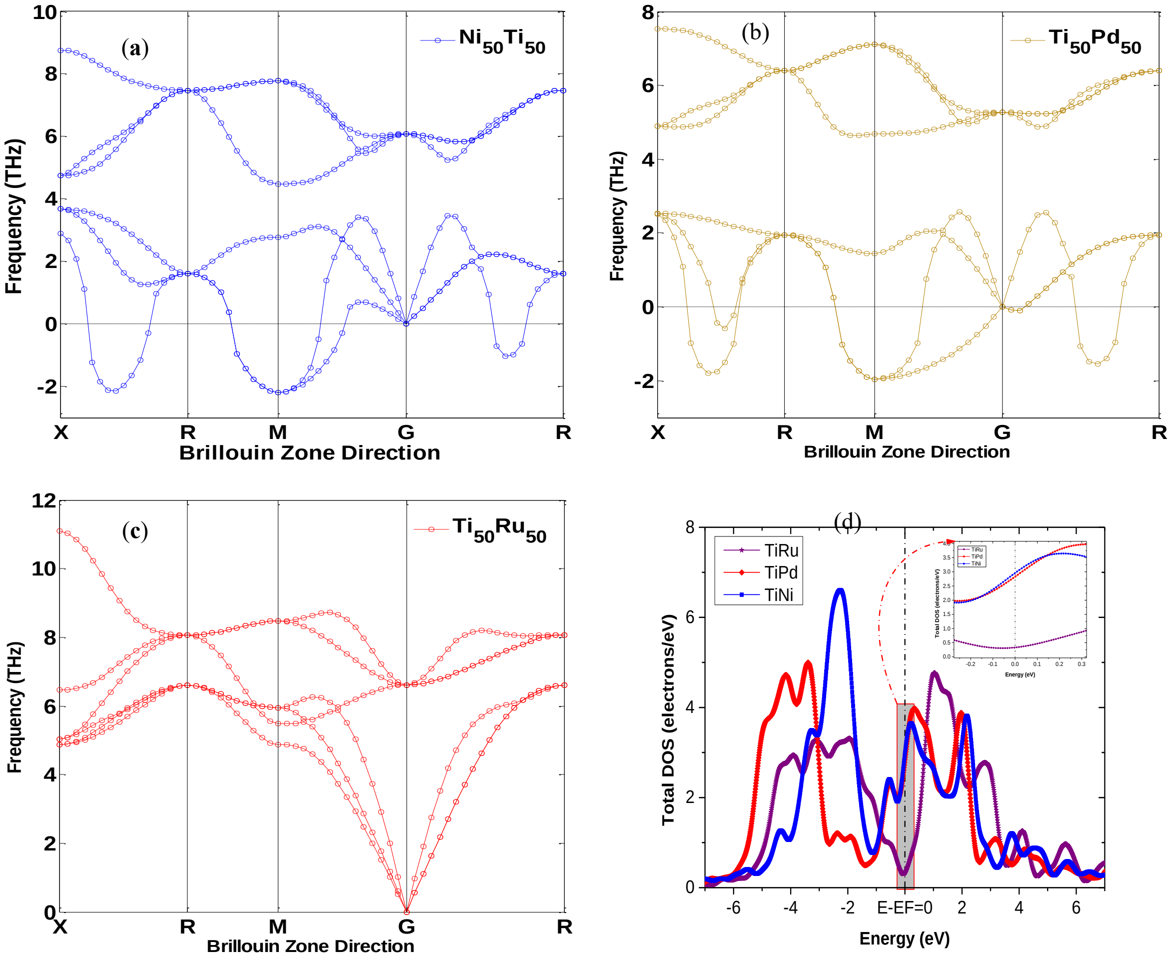

**Figure 2**. Phonon dispersion curves plotted along selected Brillouin zone labelled (a) to (c), as well as the TDOS (d) of the investigated B2 compounds.

Figure 2 (d) shows the total density of states of the three investigated CsCl compounds reported in this study. TDOS represented in Figure 2 (d) shows that B2 $Ti_{50}Ru_{50}$ remain stable down to ambient temperature with no possibility of phase transformation. This is indicated by its Fermi level ($E-E_F=0$) that cuts the deep valley (pseudogap) at the centre. In the very same Figure 2 (d), one can also observe that both $Ti_{50}Ni_{50}$ and $Ti_{50}Pd_{50}$ were found to be unstable at lower temperatures, their Fermi level was found to have shifted towards the bonding region and cuts the pseudogap on the rising shoulder. The aforementioned demonstrate that the high symmetry B2 phases of $Ti_{50}Ni_{50}$ and $Ti_{50}Pd_{50}$ cannot maintain their high symmetry at a lower temperature, it, therefore, undergo martensitic phase transition accompanied by shape memory effect.

## 4. Conclusions

The DFT model used to study the phase, mechanical and electronic stability of the investigated CsCl compounds show great reliability of the approach carried. This was indicated by the lattice parameters and heats of formation results found to be in good agreement with the available theoretical and experimental. The calculated heats of formation for all the B2 compounds were found to be thermodynamically stable. This study further finds $Ti_{50}Ru_{50}$ adheres to the mechanical stability criteria ($C_{11}>C_{12}$), while $Ti_{50}Pd_{50}$ did not adhere to the criteria an indication of phase transition of HTSMA type. The TDOS results obtained show that $Ti_{50}Ru_{50}$ to be stable as its Fermi level coincides with the centre of the pseudogap, while that of $Ti_{50}Pd_{50}$ was found to have shifted towards the bonding state, signifying the stability and instability of the B2 phases at 0 K, respectively. Furthermore, the phase stability of the B2 compounds was validated and verified through phonon vibrational frequencies.

$Ti_{50}Ru_{50}$ was found to be stable with only the positive vibrational frequency, while $Ti_{50}Pd_{50}$ presented both positive and negative frequencies, an indication of instability of the B2 phase at low temperatures.

## Acknowledgements

This paper is published with the permission of MINTEK and The University of the Witwatersrand. The authors would like to thank the Advanced Metals Initiative (AMI) of the Department of Science and Innovation (DSI) for financial support. Finally, the gratitude is also extended to the Centre for High-Performance Computing (CHPC) in Cape Town for allowing us to carry out the calculations using their remote computing resources.

## References

1. A. Wadood, *Higher Education Commission*, 1-144 (2018)
2. A. Wadood, *Adv. Mate. Sci. Eng*. **2016**, 1-9 (2016)
3. W. Bao, D. Liu, Y. Duan, M. Peng, *Philos. Mag*. **99**, 1-22 (2019)
4. S.E. Kulkova, D.V. Valujsky, *J. Phys. IV* **11**, 53-58 (2001)
5. S.E. Kulkova, D.V. Valujsky, J. S. Kim, G. Lee, Y.M. Koo, *Solid State Commun*. **119**, 619-623 (2001),
6. V. Khachin, *Rev. Phys. Appl*. **24**, 733-739 (1989)
7. H. Donkersloot, J. V. Vucht, *J. Less-Common. Met*. **20**, 83-91 (1970)
8. W.W. Xing, X. Q. Chen, D.Z. Li, L.Y. Li, C.L. Fu, *Intermetallics*. **28**, 16-24 (2012)
9. E. Semenova, *Powder. Metall. MCeram*. **36**, 394-404 (1997)
10. Z.Z. Kong, Y.H. Duan, M.J. Peng, D.Y. Qu, L.K. Bao, *Physica. B: Cond. Matter*. **573**, 13-21 (2019)
11. R. John, H. Ruben, *Mater Sci. Appl*. **2**, 1355-1366 (2011)
12. M.D. Segall, J.D.L. Philip, M.J. Probert, C.J. Pickard, P.J. Hasnip, S.J. Clark, M.C. Payne, *J. Phys. D: Condens. Matter*. **14**, 2717-2744 (2002)
13. S.J. Clark, M.D. Segall, C.J. Pickard, P.J. Hasnip, M.I. Probert, K. Refson, M.C. Payne, *Z. Kristallogr*. 220, 567–570 (2005)
14. D. Vanderbilt *Phys. Rev. B*, **41**, 7892-7895 (1990)
15. J.P. Perdew, Y. Wang, *Phys. Rev. B* **45**, 13244-13249 (1992)
16. J. P. Perdew, K. Burke, M. Ernzerhof, *Phys. Rev. Lett*. **77**, 3865 (1996)
17. T. Fischer, J. Almlof, *J. Phys. Chem*. **96**, 9768-9774 (1992)
18. F. Yu, Y. Liu, *Computations* **7** (57), 1-14 (2019)
19. E. Jain, G. Pagare, S.S. Chouhan, S.P. Sanyal, *Intermetallics* **54,** 79-184 (2014)
20. X.Q. Chen, C.L. Fu, J.R. Morris, *Intermetallics* **18**, 998-1006 (2010)
21. R. Jaradat, M. Abu-Jafar, I. Abdelraziq, A. Mousa, T. Ouahrani, R. Khenata, *AIP Adv*. **8**, 1-20 (2018)
22. J. Yang, J.H. Huang, Z. Ye, D.Y. Fan, S.H. Chen, Y. Zhao, *Ceram Int*. **43,** 7751-7761 (2017)
23. J. Jung, G. Ghosh, G. Olson, *Acta Mater*. **51**, 6341-6357 (2003)
24. J.G. Gachon, N. Selhaoui, B. Aba, J. Hertz, *J. Phase Equilibria* **13**, 506-511 (1992)
25. S. Liu, C. Tang, Y. Zhan, *Metall Mater Trans* A **47**, 1451–1459 (2016)
26. S.C. Wu, G.H. Fecher, S.S. Naghavi, C. Felser, C. *J. Appl. Phys*. **128** (8), 1-18 (2019)
27. O. Gomisa, F.J. Manjónb, P. Rodríguez-Hernándezc, A. Muñozc, *J. Phys. Chem. Solids*, **124,** 111-120 (2019)
28. M. Wagner, W. Windl, *J.* Acta Mater. **56**, 6232-6245 (2008)
29. P. Sedlák, M. Janovská, L. Bodnárová, O. Heczko, H. Seiner, *Metals* **10** (1383), 1-13 (2020)
30. L. Si, Z.-Y. Jiang, B. Zhou, W.-Z. Chen, *Phys. B* **407**, 347-351 (2012)
31. A. Togo, I. Tanaka, *Scri. Mater*. 108, 1-5 (2015